

EXPLORING CARBONATION-INDUCED VOLUME CHANGES AND THEIR RELATIONSHIP TO MICROSTRUCTURE DEVELOPMENT IN REACTIVE MAGNESIA CEMENT

QUIATCHON, P.R. *, QIU, J. *

*Department of Civil and Environmental Engineering, The Hong Kong University of Science & Technology

Email: cejqiu@ust.hk, prjquiatchon@connect.ust.hk

Key words: Reactive Magnesia Cement, Carbonation, Unrestrained Length Change

Abstract: Reactive magnesia cement (RMC) hardens through hydration and carbonation, where it sequesters CO₂ from the air. The hydration and carbonation of RMC is an intrinsically volume-expansion process. A sample calculation for the changes in molar mass and molar volume during hydration and carbonation is provided below. The hydration product, brucite undergoes carbonation and forms hydrated magnesium carbonates (HMCs), which is the primary contributor to the strength of carbonated cement. This work studies and quantifies the effect of carbonation on the volume change of RMC. The development of the microstructure over time, as it relates to volume change, was examined. Reactive magnesia cement (RMC) paste, without any additives, typically undergoes setting in 2 hours or less. The length at final setting was used as the reference point for measuring length change. After demoulding at final setting, the RMC paste was cured in a high humidity chamber for 24 hours before undergoing accelerated carbonation (10% CO₂, 23C, 85%RH). The length of the RMC specimens was measured at days 1, 3, 5, 7, 14, and 28 to quantify the volume change due to carbonation. The effect of factors such as Water-to-cement ratio, and Hydration agent were explored.

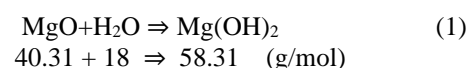
1 INTRODUCTION

During the hydration process, concrete undergoes dimensional changes that can be attributed to factors such as self-desiccation and water loss. However, excessive dimensional changes, particularly in restrained members, can have detrimental effects on the structure. Such changes can lead to micro-cracking, which serves as an entry point for deleterious substances [1-3], or substantial cracks that can cause structural instability.

Ordinary Portland Cement, the traditional binder used to mix concrete, experiences dimensional changes due to self-desiccation and drying [4-5]. To address this problem, researchers have tried to tailor the mix design by adjusting the water-to-cement ratio [6] or

through the addition of shrinkage-reducing admixtures [7-9].

However, environmental concerns regarding OPC's CO₂ emissions during its manufacturing process has pushed researchers to look for more sustainable cementitious binders. Reactive Magnesium Oxide (rMgO) cement is a promising alternative to OPC because of its ability to sequester and mineralize carbon dioxide [10]. The strength-gain mechanism of MgO is a two-step process: hydration (**Eq.1**) and carbonation (Eq.2). MgO hydration produces brucite (Mg(OH)₂), accompanied by a ~127% increase in solid volume.



$$11.2 + 18 \Rightarrow 25.3 \text{ (cm}^2\text{)}$$

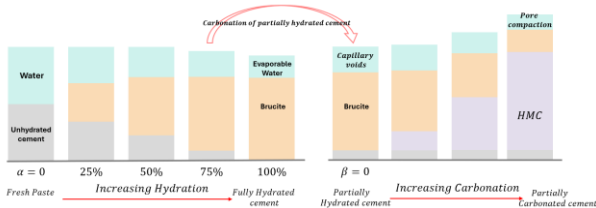
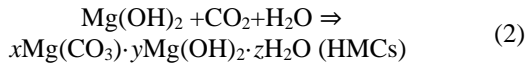


Figure 1. Formation of Hydration and Carbonation product and their effect on the total volume

2 MATERIALS AND METHODS

2.1. Material Characterization

This study used two groups of RMC specimens that were grouped based on how factors affect early hydration. Hydration agent was added at a constant water-to-cement ratio of 0.8.

| | Proportions by mass of RMC | | | HA (M) ^a |
|-----------------|----------------------------|-----|-------|---------------------|
| | Mix ID | RMC | Water | |
| RMC Paste | RMC-0.7 | 1.0 | 0.7 | - |
| | RMC-0.8 | | 0.8 | - |
| | RMC-0.9 | | 0.9 | - |
| Hydration Agent | 0.05M | 0.8 | 0.8 | 0.05M |
| | 0.1M | | 0.8 | 0.1M |

Reactive MgO was obtained from Konoshima Chemical Co. Ltd. An SEM image of the particle is shown in Figure 2.

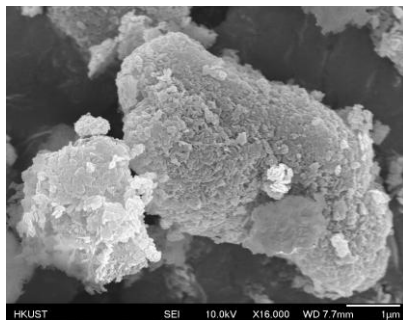


Figure 2. SEM image of rMgO

The reactivity of the rMgO was measured using an acetic acid test and found to be about 7.5s [11]. The particles have an irregular shape and surface area, with a mean size of 5.5 µm

(Figure 3). This MgO is more reactive than the rMgO used in existing literature and is expected to hydrate quickly.

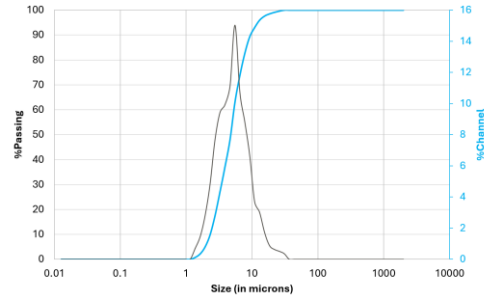


Figure 3. Particle size distribution of RMC

An X-ray diffraction analysis of the MgO used is shown in Figure 4, with the highest peak occurring at 42.9°, followed by peaks at 62.48°, 78.60° and 36.93°.

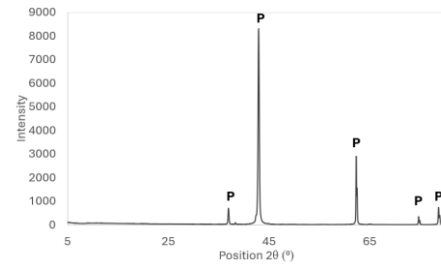


Figure 4. XRD of Reactive MgO

The Magnesium Acetate (MA) solution was acquired from Sigma-Aldrich and used as a hydration agent.

2.2. Linear dimensional measurements

To ensure uniform carbonation throughout the entire depth of the specimen, a special mould was prepared for linear dimensional measurements, following the aspect ratio specified in ASTM C157/C157M (2017). Small cylindrical samples measuring 10 mm in diameter and 100 mm in length were chosen for this purpose.

The length and mass at final setting were used as the reference points for measuring length change. After demoulding at final setting, the RMC paste was cured in a high-humidity chamber (99%) for 24 hours before placing the specimens in two curing

conditions: accelerated carbonation C10 (10% CO₂, 85% RH, 23°C) and Ambient (0.04% CO₂, 60% RH, 23°C). Mass and length measurements were taken on days 1, 3, 5, 7, 14, 21, and 28.

2.3. Compressive Strength Test

Cube specimens (20 mm) were prepared and demoulded after 24 hours. They were then cured under two different conditions: C10 (10% CO₂, 85% RH, 23°C) and Ambient (0.04% CO₂, 60% RH, 23°C). Before testing the cubes, the mass and volume were measured for density calculations. Testing was performed on days 3, 7, 14, and 28 at a rate of 0.05 mm/min.

2.4. Microstructural Investigation (SEM)

For microstructural analysis, additional 10 mm cubes were prepared. At the desired age, these cubes were polished using 400, 1200, and 2000 mesh sandpaper, then submerged in isopropyl alcohol for 7 days and vacuum-dried immediately afterward. The microstructures of the prisms were examined using a scanning electron microscope (SEM, JEOL-6390).

3 RESULTS AND DISCUSSION

3.1. Linear dimensional measurements

Figure 7 presents a representative graph of the length and mass changes of RMC-0.8. The cylinders subjected to accelerated carbonation curing exhibited increases in both mass and volume. Length changes during accelerated carbonation were predominantly positive but did not show exponential growth, stabilizing within 200 microns. In contrast, the cylinders cured in ambient conditions were significantly affected by moisture fluctuations, with shrinkage primarily attributed to drying. However, from day 21 to day 28, there was a slight increase in length (approximately 100 microns). This change is not due to carbonation as there is no increase in mass but may result from the rebound of surface tension

following the partial evaporation of water from the capillary pores.

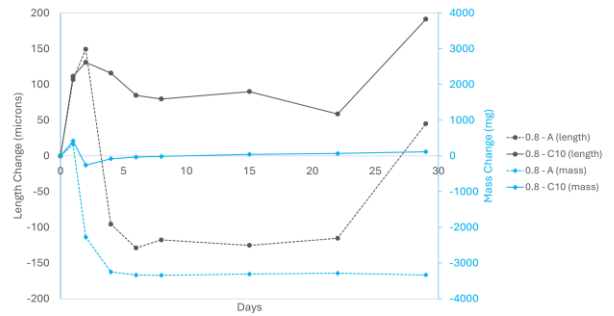


Figure 5. Length and Mass change of RMC-0.8 (Carbonated and Ambient cured) for 28 days

Figure 7 represents the general behaviour of all RMC in the mix design

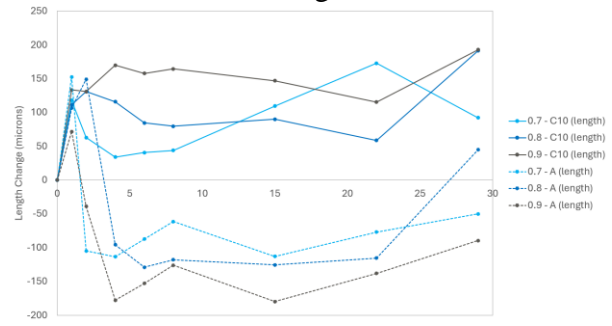


Figure 6. Effect of water-to-cement ratio on unrestrained length change of RMC

Figure 8 shows the effect of carbonation on the unrestrained length change of RMC with varying water-to-cement ratios. The mix with the highest water content exhibited the greatest expansion in the C10 (10% Carbonated) group and the most significant shrinkage in the A (Ambient) group. The lowest water-to-cement ratio (RMC-0.7) showed minimal expansion and only slight shrinkage over time, likely due to its initially compact microstructure. In contrast, RMC-0.8 experienced expansion in both ambient and carbonated conditions. This may be attributed to the capillary porosity and voids in this paste, which facilitated CO₂ penetration in the C10 group (similar to RMC-0.9), while the water content was not excessively high, resulting in minimal shrinkage in ambient curing.

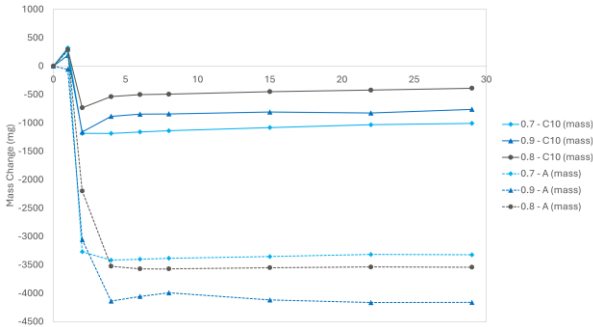


Figure 7. Effect of water-to-cement ratio on mass change of RMC

The change in mass exhibits a trend similar to that of the unrestrained length change. The RMC-0.8 mix shows the greatest change in mass. As previously mentioned, the void ratio in this mix may be optimal for maximizing carbonation while minimizing shrinkage. RMC-0.9 recorded the second highest mass gain during carbonation but experienced the largest mass loss in ambient conditions due to its voids. In contrast, RMC-0.7 had the lowest increase in mass within the carbonated group and exhibited minimal shrinkage in ambient conditions compared to the other water-to-cement mixes, likely due to its compact microstructure.

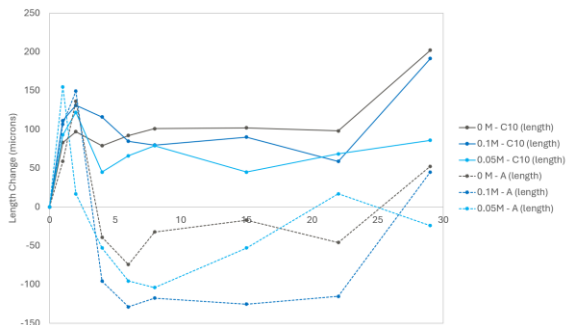


Figure 8. Effect of Hydration agent on unrestrained length change of RMC

The highest length gain in the carbonated samples was observed in the 0M and 0.1M mixes (Figure 10). Notably, the 0.1M mix experienced the greatest shrinkage while also exhibiting the highest degree of "bounce-back." The efficiency of converting MgO to brucite in the 0.1M mix is evident from the mass change observed in the ambient environment (Figure 11). Instead of water evaporating and causing mass loss and shrinkage, it was consumed by MgO for

hydration, which explains the minimal mass loss alongside significant shrinkage. In the carbonated group, the 0.1M mix showed the second highest expansion, following the 0M mix. This may be attributed to the efficiency of hydration, which made the microstructure more compact and less conducive to carbonation.

Finally, the 0.5M mix showed significant stability, experiencing the least expansion in the carbonated environment and lacking the "bounce-back" effect observed in the 0M and 0.1M mixes.

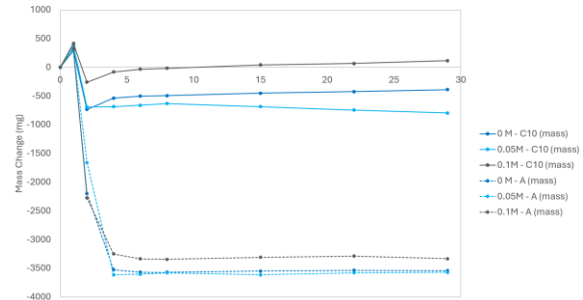


Figure 9. Effect of Hydration agent on unrestrained mass change of RMC

3.2. Compressive Strength

Figure 10 illustrates the effect of the water-to-cement ratio and carbonation curing. As the duration of carbonation curing increases, the compressive strength of the cubes also rises. An inverse correlation exists between early strength and water content, which is expected since a higher water-to-cement ratio results in more capillary pores.

For cubes cured in an ambient environment, the strength plateaus around day 14, with compressive strengths on days 14 and 28 being nearly equal. In contrast, for cubes subjected to accelerated curing, the compressive strength continues to increase up to day 28. With longer curing periods, we anticipate that strength will keep rising as hydrated magnesium carbonates (HMC) continue to fill the capillary pores and voids in specimens with a high water-to-cement ratio.

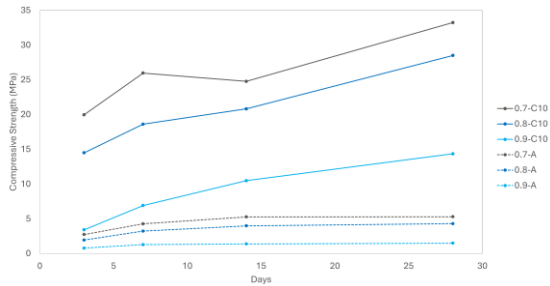


Figure 10. Effect of Water-to-cement ratio and curing on Compressive Strength

The impact of adding a hydration agent and the effects of carbonation curing on compressive strength is evident as shown in Figure 13. Longer carbonation curing resulted in higher compressive strength. The addition of 0.05M to the mix had minimal effect, as the development of compressive strength for both the control sample and the 0.05M cubes in both curing conditions was nearly identical.

In contrast, the incorporation of a hydration agent at 0.1M significantly enhanced the early-age compressive strength in both carbonated and ambient conditions. The strength of the C10-0.1M cubes increased by 167% from day 3 to day 7, and by 55% from day 7 to day 28. The compressive strength continued to rise and is expected to increase beyond day 28.

Unlike pure RMC paste, which plateaus at day 14, the addition of the 0.1M hydration agent resulted in a continuous increase in compressive strength from day 14 to day 28. Furthermore, the 28-day strength of the 0.1M cubes is 122% higher than that of the 0M specimens, highlighting the positive effect of the hydration agent. Hydration continues beyond day 14.

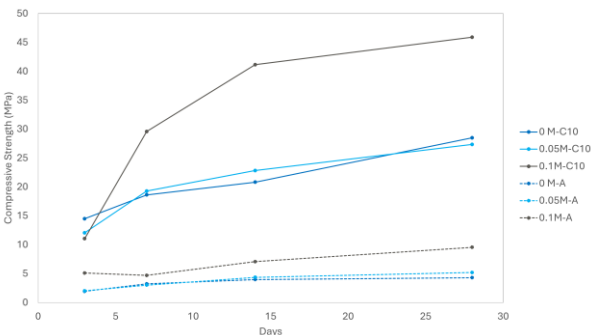


Figure 11. Effect of Hydration agent and curing on Compressive Strength

Figures 14 and 15 compare the strength and density of Reactive Magnesia Cement (RMC) with varying water-to-cement ratios and different hydration agent contents. There is a direct relationship between the strength and density of the RMC cubes. In Figure 14, the cubes with a water-to-cement ratio of 0.7 exhibit the highest density and compressive strength, followed by those with ratios of 0.8 and 0.9, respectively.

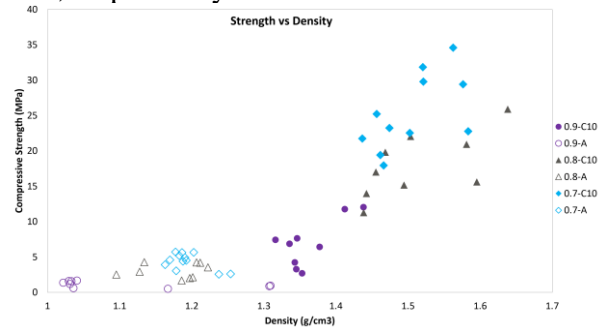


Figure 12. Compressive Strength vs Density of RMC paste with varying w/c ratio

Figure 15 shows that RMC cubes containing 0.1M of the hydration agent achieve the highest compressive strength and density, while the cubes with 0M and 0.05M hydration agent have similar values.

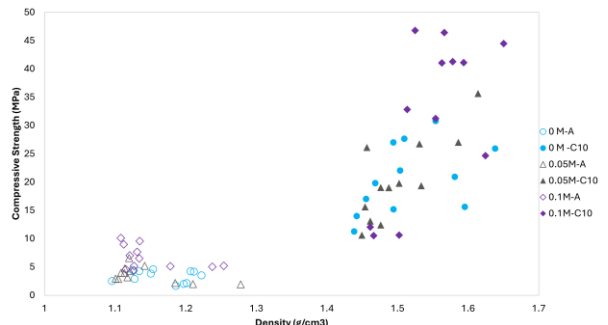


Figure 13. Compressive Strength vs Density of RMC paste with varying hydration agent content

3.3. Microstructural Investigation

Microstructural analysis of RMC-0.8 was performed at the initial and final setting times. Figures 16 and 17 illustrate that brucite began to nucleate on the MgO grains during both the initial and final setting times. Distinct clusters of brucite flakes are clearly visible at the final setting time. Although brucite flakes can be observed, the shape of the MgO grains remains prominent. By day 14, the micrograph reveals that the RMC is predominantly covered by

brucite flakes, making the MgO grains less discernible.

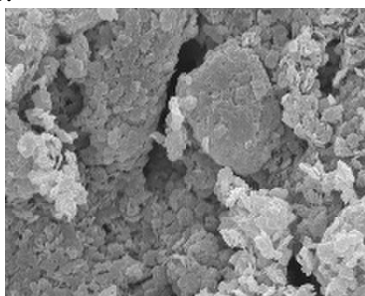


Figure 14. SEM of brucite on MgO at initial setting time

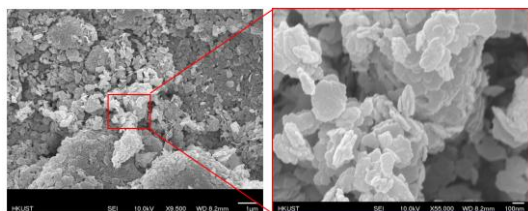


Figure 15. Formation of brucite at final setting time

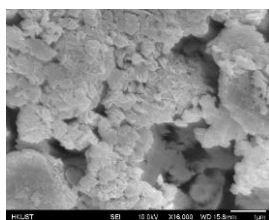


Figure 16. SEM of Ambient cured RMC (day 14)

Needle-like structures, believed to be nesquehonite, were observed in RMC-0.7 on day 3. HMC formation is expected as the difference in compressive strength for ambient and carbonated group is quite significant even at an early age. The 3-day compressive strength of the carbonated cubes is 628% higher than that of the ambient-cured cubes.

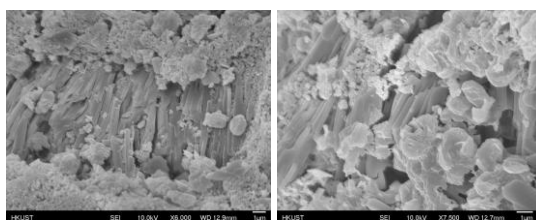


Figure 17. SEM of Day 3 Carbonated RMC-0.7

12 CONCLUSIONS

The unrestrained length change and compressive strength of Reactive Magnesia Cement (RMC) mixes with varying water-to-cement ratios and hydration agent contents were examined, with a focus on the impact of

carbonation curing in relation to these factors. The water-to-cement ratio significantly influences length change due to the formation of pores resulting from the evaporation of unconsumed water, which serve as pathways for CO₂ to penetrate and carbonate the hydration products.

The addition of a hydration agent notably affected the development of final compressive strength in both carbonated and ambient-cured samples. Among the mixes, the 0.1M hydration agent had the most pronounced impact on hydration and carbonation. It promoted the formation of brucite, resulting in a denser microstructure that enhanced the compressive strength of the ambient-cured samples. This mix effectively converted a substantial amount of MgO into brucite, thereby facilitating the subsequent formation of hydrated magnesium carbonates (HMC).

REFERENCES

1. Djerbi, A., Bonnet, S., Khelidj, A., & Baroghel-bouny, V. (2008). Influence of traversing crack on chloride diffusion into concrete. *Cement and Concrete Research*, 38(6), 877–883. <https://doi.org/10.1016/j.cemconres.2007.10.007>
2. Gérard, B., & Marchand, J. (2000). Influence of cracking on the diffusion properties of cement-based materials. *Cement and Concrete Research*, 30(1), 37–43. [https://doi.org/10.1016/S0008-8846\(99\)00201-X](https://doi.org/10.1016/S0008-8846(99)00201-X)
3. Mangat, P. S., & Gurusamy, K. (1987). Permissible crack widths in steel fibre reinforced marine concrete. *Materials and Structures*, 20(5), 338–347. <https://doi.org/10.1007/BF02472580>
4. Craipeau, T., Perrot, A., Toussaint, F., Huet, B., & Lecomte, T. (2021). Mortar pore pressure prediction during the first hours of cement hydration. *Cement and Concrete Composites*, 119, 103998. <https://doi.org/10.1016/j.cemconcomp.2021.103998>

5. Hansen, W. (1987). Drying Shrinkage Mechanisms in Portland Cement Paste. *Journal of the American Ceramic Society*, 70(5), 323–328. <https://doi.org/10.1111/j.1151-2916.1987.tb05002.x>
6. Kioumars, M., Azarhomayun, F., Haji, M., & Shekarchi, M. (2020). Effect of Shrinkage Reducing Admixture on Drying Shrinkage of Concrete with Different w/c Ratios. *Materials*, 13(24), 5721. <https://doi.org/10.3390/ma13245721>
7. Dang, Y., Qian, J., Qu, Y., Zhang, L., Wang, Z., Qiao, D., & Jia, X. (2013). Curing cement concrete by using shrinkage reducing admixture and curing compound. *Construction and Building Materials*, 48, 992–997. <https://doi.org/10.1016/j.conbuildmat.2013.07.092>
8. Mora-Ruacho, J., Gettu, R., & Aguado, A. (2009). Influence of shrinkage-reducing admixtures on the reduction of plastic shrinkage cracking in concrete. *Cement and Concrete Research*, 39(3), 141–146. <https://doi.org/10.1016/j.cemconres.2008.11.011>
9. Zhan, P., & He, Z. (2019). Application of shrinkage reducing admixture in concrete: A review. *Construction and Building Materials*, 201, 676–690. <https://doi.org/10.1016/j.conbuildmat.2018.12.209>
10. Unluer, C. (2018). Carbon dioxide sequestration in magnesium-based binders. In *Carbon Dioxide Sequestration in Cementitious Construction Materials* (pp. 129–173). Elsevier. <https://doi.org/10.1>
11. Shand, M. A. (2006). *The chemistry and technology of magnesia*. Wiley-Interscience.